Modelling of Surface Reactions for Predicting Dry-Etched Profiles

K. Harafuji, A. Misaka, M. Kubota and N. Nomura

Semiconductor Research Center, Matsushita Electric Ind. Co., Ltd.,
3-1-1 Yagumo-Nakamachi, Moriguchi, Osaka 570, Japan

Introduction

A key step in dry etching is the reaction occurring at the surface. There have been several attempts in the past to predict the evolution of etching profile and maintain consistency in designed dimensions. Earlier models for simulation of dry etching, however, have had difficulty in describing the surface processes, since reaction rates are evaluated only by incoming ion/radicals. In this work, we propose a simulation model for surface reaction by considering competing mechanisms involving simultaneous deposition and etching. We consider the interaction between incoming ion/radicals and a dynamic surface condition.

Surface Reaction Model

Surface conditions are described by taking into account an adsorbed particle layer on the substrate surface. For this purpose, we introduce a concept of "infinitesimal reaction surface"(IRS) as shown in Fig.1[1-4]. Substrate surface is divided into number of small areas. On each small area or IRS, different kinds of radicals are adsorbed just like mosaic. Here, AS^k and ES are defined as the coverage ratio of adsorbed particle k and that by clean substrate surface on IRS, respectively, where the following conditions are imposed:

$$\sum_k AS^k + ES = 1, \quad \sum_k AS^k \geqq 0, \quad ES \geqq 0 \quad (1)$$

For simplicity, only two kinds of reactive radicals kr (denoted by black) and non-reactive radical kn (denoted by gray) are adsorbed in Fig.1.

Different reaction processes proceed on different adsorbed particle layer surfaces. On the reactive radical layer surface, ion-assisted etching under ion bombardment as well as thermally-induced chemical reaction take place. On the non-reactive radical layer surface, deposition process proceeds and etching is much inhibited. On the clean substrate surface, ion-sputtering etching occurs. Etching rate is expressed by the summation of these reactions on different particle layer surfaces whose ratios are denoted by AS^k and ES. Thus, the IRS gives the base for describing averaged reaction phenomena on each position r of the substrate surface.

Fig.2 shows the flowchart of the present simulation model. Real time T with finite time step ΔT is advanced to obtain new surface topology. First, simultaneous equations (2) are solved to obtain radical flux $F^m(r)$ of particle m on each position r,

$$F^m(r) = F^m_{dir}(r) + \int K(r,r')(1-\sigma^m)\, F^m(r')dr' \quad (2)$$

Here, $F^m{}_{dir}(r)$ is the direct flux; the second term in the right hand side denotes self-consistent re-emission radical flux due to finite sticking coefficient under the IRS theory[3,5]; $K(r,r')$ is the kernel describing the geometrical relation between r and r'; and σ^m is the sticking coefficient of particle m. This is schematically shown in Fig.3. AS^m and ES are determined by the balance between adsorption and desorption rate of particle m as shown in Fig.4. The following differential equations are solved to obtain stationary values of AS^m and ES,

$$\frac{d}{dt}AS^m = L\left[\, G^m(r,T) - H^m(r,T) \,\right] = 0 \quad (3)$$

$$\frac{d}{dt}ES = \sum_m L\left[\, H^m(r,T) - G^m(r,T) \,\right] = 0 \quad (4)$$

where t is an artificial time, L is a constant proportional to the inverse of inter-atomic length of adsorbed particle m. G^m is the number of adsorbing partcles per unit time, H^m is the number of desorbing partcles per unit time, and these are described by

$$G^m = \sigma^m \cdot F^m(r) = \left[\, \sum_k \sigma^{mk} \cdot AS^k + \sigma^{me} \cdot ES \,\right] \cdot F^m(r) \quad (5)$$

$$H^m = h \cdot AS^m \quad (6)$$

where σ^{mk} and σ^{me} are elemental sticking coefficients of particle m on the adsorbed layer of particle k and on the clean substrate, respectively, and h is the desorbing rate of adsorbed particle m. An example of time dependent surface condition is shown in Fig.5.

Etching rate vector $\mathbf{E}(t,r)$ or deposition rate vector $\mathbf{D}(r,t)$ is calculated for the substrate material as follows:

$$\mathbf{E}(r,T) = \sum_k \mathbf{E}^{ke}_{\mathrm{cr}} \cdot AS^k + \sum_i \sum_k \mathbf{E}^{ike}_{ast} \cdot AS^k + \sum_i \mathbf{E}^{ie}_{spt} \cdot ES \quad (7)$$

$$\mathbf{D}(r,T) = \sum_k (G^k - H^k) \cdot \mathbf{n} \qquad (8)$$

Here, $\mathbf{E}_{cr}$, $\mathbf{E}_{spt}$ and $\mathbf{E}_{ast}$ are elemental etching rate vectors of the chemical reaction, the ion-sputtering and the ion-assisted etching, respectively. $\mathbf{n}$ is the normal unit vector to the surface. Suffix i and e designate impinging ions and substrate materials, respectively. If ES is greater than 0, then an etching process is predicted. If ES is 0, then a deposition process is predicted (see Fig.1).

Simulation Results

A. Simulation Model

Silicon-dioxide etching by hydrofluorocarbon gas was examined. Two kinds of radicals [F] and [$C_mH_nF_x$], and ions dissociated from C-H-F compounds produced in plasmas are considered, and these fluxes transported on the surface are denoted by N_F, N_{CHF} and Ni, respectively. Enhanced ion-assisted etching occurs for both kinds of adsorbed radicals when there is simultaneous energetic ion bombardment. The adsorbed [$C_mH_nF_x$] radicals result in polymer deposition, when there is no ion bombardment. Unknown parameters of sticking coefficients and radical/ion fluxes are estimated *a priori* by fitting a profile to an experiment in an overhang test structure[3,6].

Angular distribution of ions is calculated by a Monte Carlo transport code in the sheath region[7]. Radicals are transported isotropically. A string model is used to express time-evolution of surface topology.

B. Application to Infinite Trench Configurations

Fig.6 shows the comparison between transported-limited and reaction-rate-limited cases by [F] radical etching[2]. Three different mask window widths, W, were examined. In Fig.6(a), radical supply is insufficient when compared with the intrinsic reaction rate with substrate material, i.e., the etching rate is limited by N_F. Anisotropic etching component appears due to a finite window angle. In Fig.6(b), there is sufficient supply of radicals, and isotropic etching proceeds. IRS is always covered with reactive [F] radicals, i.e., $AS^F = 1.0$, $ES = 0$. The etching rates at the bottom are almost identical, even when W is varied. Etching rate is limited by the reaction-rate.

Fig.7 shows microloading effects[4]. Mask width W and the ratio of N_F/N_i are varied. In this case, ion-assisted etching is the dominant mechanism. The etching rate is dependent on the coverage ratio AS^F as well as ion flux. As W decreases, the etching rate becomes smaller. This is because the number of directly transported radicals on the trench bottom is smaller. This phenomena is more typical when N_F/N_i is smaller.

Fig.8 shows the competition phenomena between etching and deposition[2]. The ratio of N_F/N_{CHF} is varied. N_F/N_i is 100. W is maintained 1.0μm. The larger value of $\alpha = N_F/N_{CHF}$ results in a bowed profile, since isotropic chemical reaction by [F] radicals becomes dominant. A vertical wall profile is realized for (b) due to the balance between etching and deposition on the side-wall. Large N_{CHF} gives a thick lateral deposition resulting in a tapered profile.

C. Comparison between Trench and Hole Geometries

Fig.9 shows comparison between experiments and simulations for trench and hole configurations[3]. Geometrical extension to hole configurations is made under the assumption of rotational symmetry. Bowed profile is more prominent for holes compared with trenches. This is because both direct and indirect depositive radical fluxes for the protection of sidewall etching decrease by the shrinkage of incoming window angle and slightly inclined ion etching (denoted by arrows) becomes more dominant. Simulation shows good match with SEM images.

Conclusion

A surface reaction model for dry-etching process, which takes ever-changing adsorbed particle layers on the substrate surface into account, was described. Silicon-dioxide etching by hydrofluorocarbon gases was treated. The present model is able to express the following etching mechanisms based on the unified IRS theory: (a)the phenomenological difference between transported-limited and reaction-rate-limited cases by radical etchings; (b)the microloading effects due to the shortage of reactive radicals on the trench bottom; (c)the competition between etching and deposition. Simulational results of surface profiles after etching show a good match with experimental data for trench/hole configurations with dimensions smaller than one micrometer.

References

[1]A.Misaka, K.Harafuji, H.Nakagawa, T.Tamaki, M.Kubota and N.Nomura, Digest of Papers Microprocess Conf. 92, 1992, pp142-143.

[2]K.Harafuji, A.Misaka, M.Kubota and N.Nomura, Shinkuu(in Japanese), vol.35, 1992, pp925-934.

[3]K.Harafuji, A.Misaka, H.Nakagawa, T.Tamaki, M.Kubota and N.Nomura, Tech. Digest 1992 IEDM, pp169-172.

[4]A.Misaka, K.Harafuji, M.Kubota and N.Nomura, Jpn. J. Appl. Phys. vol.31, 1992, pp4363-4369.

[5]M.Mazhar IslamRaja, M.A.Cappelli, J.P.McVittie and K.C.Saraswat, J. Appl. Phys. vol.70, 1991, pp7137-7140.

[6]J.P.McVittie, J.C.Rey, A.J.Banya, M.M.IslamRaja, L.Y.Cheng, S.Ravi and K.C.Saraswat, Proc. SPIE Symp. vol.1392, 1990.

[7]J.I.Ulacia F. and J.P.McVittie, J. Appl. Phys. vol.65, 1989, pp1484-1491.

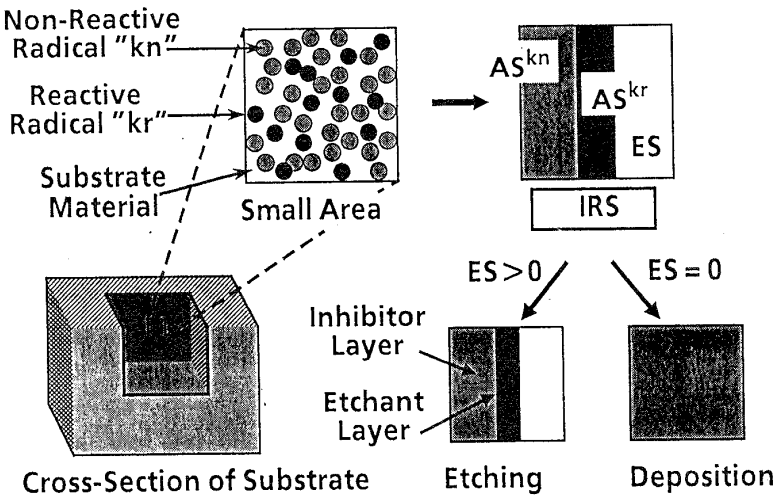

Fig.1 A concept of "infinitesimal reaction surface"(IRS). AS^k and ES are coverage ratios of radical k and substrate material on IRS, respectively. If ES on IRS is greater than 0, then etching process occurs. If ES is 0, then deposition process occurs.

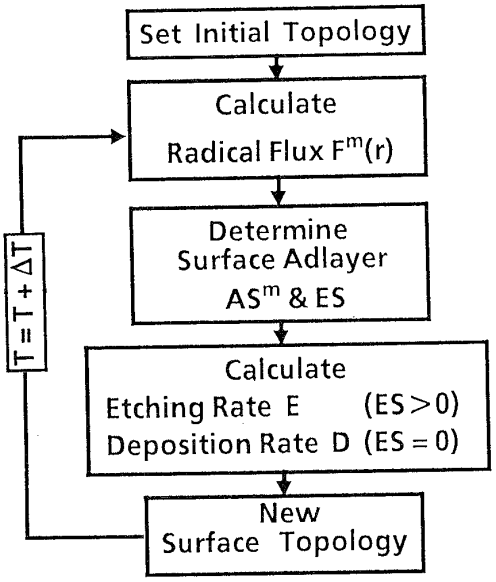

Fig.2 Flowchart of the present simulation model.

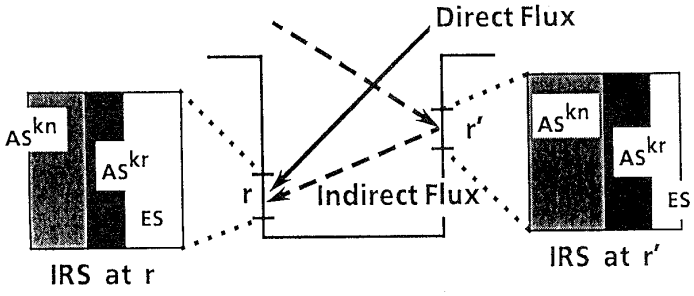

Fig.3 A model for calculating total flux at r. The total flux is composed of direct flux and re-emission indirect flux.

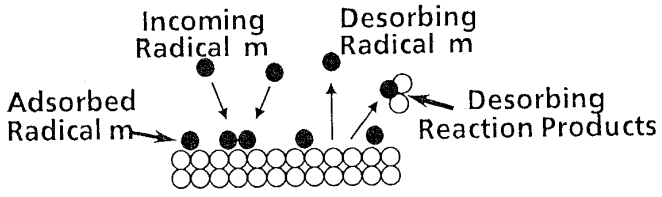

Fig.4 A surface reaction model to determine AS^m and ES.

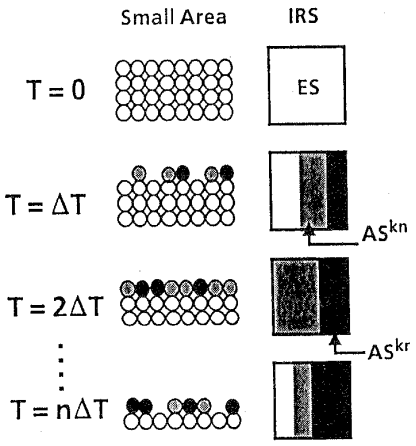

Fig.5 Time-evolution of adsorbed particles on the substrate in the small area. Corresponding AS^k and ES on IRS are also shown.

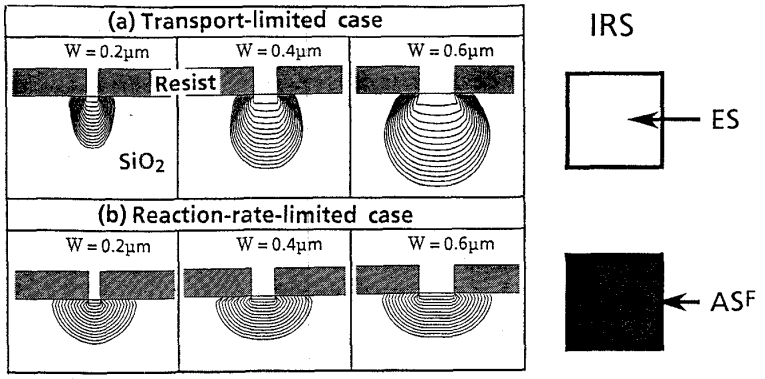

Fig.6 Comparison between transport-limited and reaction-rate-limited cases in trench etching by [F] radicals. IRS at the trench bottom is also schematically shown on each case.

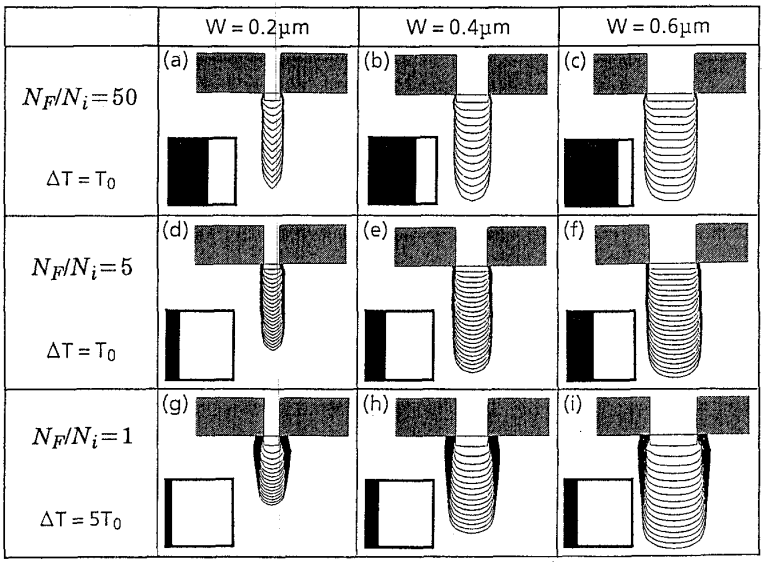

Fig.7 Microloading effect in trench etching. Mask width W and N_F/N_i are varied. IRS at the trench bottom is also schematically shown on each case. Time step ΔT for (g), (h) and (i) is five times larger than that for the other cases.

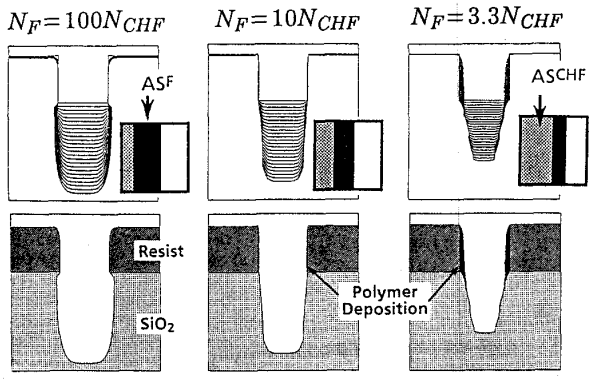

Fig.8 Competition between etching and deposition on the side-wall in trench etching. $W=1.0\mu m$. N_F/N_i is 100. N_i is fixed. IRS on the side wall is also schematically shown on each case.

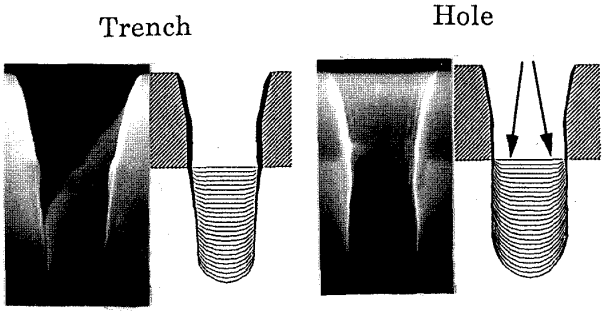

Fig.9 Comparison between simulations and experiments for infinite-trench and hole etchings. $W=0.6\mu m$. $N_F/N_i=83$. $N_{CHF}/N_i=2.5$.